Experimental and Theoretical Analysis of the Invasive Signal Amplification Reaction†

Victor I. Lyamichev,*,‡ Michael W. Kaiser,‡ Natasha E. Lyamicheva,‡ Alexander V. Vologodskii,§ Jeff G. Hall,‡ Wu-Po Ma,‡ Hatim T. Allawi,‡ and Bruce P. Neri‡

Third Wave Technologies, Inc., 502 South Rosa Road, Madison, Wisconsin 53719-1256, and Department of Chemistry, New York University, 31 Washington Place, New York, New York 10003

Received April 5, 2000; Revised Manuscript Received May 31, 2000

ABSTRACT: The invasive signal amplification reaction is a sensitive method for single nucleotide polymorphism detection and quantitative determination of viral load and gene expression. The method requires the adjacent binding of upstream and downstream oligonucleotides to a target nucleic acid (either DNA or RNA) to form a specific substrate for the structure-specific 5′ nucleases that cleave the downstream oligonucleotide to generate signal. By running the reaction at an elevated temperature, the downstream oligonucleotide cycles on and off the target leading to multiple cleavage events per target molecule without temperature cycling. We have examined the performance of the FEN1 enzymes from *Archaeoglobus fulgidus* and *Methanococcus jannaschii* and the DNA polymerase I homologues from *Thermus aquaticus* and *Thermus thermophilus* in the invasive signal amplification reaction. We find that the reaction has a distinct temperature optimum which increases with increasing length of the downstream oligonucleotide. Raising the concentration of either the downstream oligonucleotide or the enzyme increases the reaction rate. When the reaction is configured to cycle the upstream instead of the downstream oligonucleotide, only the FEN1 enzymes can support a high level of cleavage. To investigate the origin of the background signal generated during the invasive reaction, the cleavage rates for several nonspecific substrates that arise during the course of a reaction were measured and compared with the rate of the specific reaction. We find that the different 5′ nuclease enzymes display a much greater variability in cleavage rates on the nonspecific substrates than on the specific substrate. The experimental data are compared with a theoretical model of the invasive signal amplification reaction.

With the advent of the genomics revolution, the need for low-cost and high-throughput methods for nucleic acid analysis has never been greater. The existing methods for nucleic acids detection can be divided into two categories: those based on target amplification, such as PCR[1] (*1*), LCR (*2*), TAS (*3*); and those based on signal amplification. The latter greatly simplify target quantitation and have the advantage of greatly reducing the possibility of cross-contamination in analyses of large numbers of samples. One approach to signal amplification, utilized by the bDNA (*4*) and hybrid capture techniques (*5*), is annealing of a sequence-specific probe to each target site followed by labeling of the resulting complex with multiple reporter molecules. In an alternative approach, called a probe cycling reaction, a sequence-specific probe can be annealed to a target sequence and then cleaved by a specific nuclease, such as RNase H (*6*), λ exonuclease (*7*), exonuclease III (*8*), or a structure-specific 5′ nuclease (*9*). In the RNase H, λ exonuclease, and exonuclease III techniques, cleavage of the bound probe destabilizes the duplex, resulting in dissociation of the cut probe, which allows an uncut probe to bind to the target sequence. In the 5′ nuclease method, rapid replacement of the cleaved probe is achieved by performing the reaction at elevated temperature. For all probe cycling techniques, dissociation of the cleaved probe and then annealing of an uncut probe are followed by further rounds of cleavage and probe replacement, thus yielding multiple cleavage events for each target molecule during the course of the reaction.

Recognition of the specific sequence of a target molecule using the structure-specific 5′ nucleases requires two oligonucleotides to anneal in an adjacent manner to the target molecule. The resulting adjacent duplexes must overlap by at least one nucleotide to create an efficient substrate, called the overlapping substrate, for the 5′ nucleases. The 5′ end of the downstream oligonucleotide, also called the probe, contains an unpaired region termed the 5′ arm (*10*) or flap (*11*) that is not required for the enzyme activity; however, very long arms can inhibit cleavage (*10*). Specific cleavage of the probe, termed invasive cleavage (*9*), occurs at the position defined by the 3′ end of the upstream oligonucle-

† This research was supported by the U.S. Department of Commerce, National Institute of Standards and Technology, Advanced Technology Program, Cooperative Agreement Number 70NANB7H3015 to Dr. Lance Fors.

* To whom correspondence should be addressed. Phone: (608) 663-7017; Fax: (608) 273-8618; E-mail: vlyamichev@twt.com.

‡ Third Wave Technologies.

§ New York University.

[1] Abbreviations: FEN1, flap endonuclease 1 enzyme; PCR, polymerase chain reaction; LCR, ligase chain reaction; bDNA, branched DNA; TAS, transcription-based amplification system; SNP, single nucleotide polymorphism; BSA, bovine serum albumin; TET, tetrachlorofluorescein; HPLC, high-performance liquid chromatography; MOPS, 4-morpholinepropanesulfonic acid; EDTA, ethylenediaminetetraacetic acid; NP-40, Nonidet P-40, T_m, melting temperature; K_d, equilibrium dissociation constant; btSA, biotin−streptavidin complex.

10.1021/bi0007829 CCC: $19.00
Published on Web 07/07/2000

otide, which displaces or "invades" the probe. If the overlap between the adjacent oligonucleotides is only one nucleotide, cleavage takes place between the first two base pairs of the probe, thus releasing its 5′ arm and one nucleotide of the base paired region (*12, 13*).

In a signal amplification modification of an invasive reaction described previously (*9, 14*), an upstream oligonucleotide and a probe are present in large molar excess over the target nucleic acid. When invasive cleavage is carried out near the melting temperature of the probe, a cut probe can rapidly dissociate, and an intact probe will anneal to the target more frequently than will a cut probe, thus initiating a new cycle of cleavage. Hence, multiple probes can be cut for each target molecule under isothermal conditions, resulting in linear signal amplification with respect to target concentration and time (*9*). Herein, we refer to this assay as the invasive signal amplification reaction. Addition of a second invasive signal amplification reaction, in which the cleaved 5′ arm from the first reaction functions as an upstream oligonucleotide in the second reaction, enables total signal amplification as great as 10^7 (*14, 15*). This level of amplification is sufficient for direct single nucleotide polymorphism (SNP) analysis on genomic DNA, quantitative analysis of viral load, and quantitative gene expression without any preliminary target amplification steps, such as PCR (*14*−*18*).

The requirement for overlap between the upstream oligonucleotide and the probe can be employed for high-level nucleotide discrimination, which is critical for SNP analysis. To accomplish this, the probe is designed so that the nucleotide immediately upstream of the cleavage site can base pair with the nucleotide of interest in the target strand. When the target and probe are complementary at the position of the polymorphism, overlap occurs between the upstream oligonucleotide and probe, resulting in efficient cleavage. When the target and probe are not complementary in this position, overlap is eliminated, and the cleavage rate is very low (*9, 13*). This large difference in cleavage rates between substrates having overlap between the upstream oligonucleotide and probe and substrates which lack overlap ensures a high level of nucleotide discrimination in SNP analysis (*9, 14, 17*−*19*).

Further improvements in the method require a detailed understanding of the invasive signal amplification reaction, including the thermodynamics and kinetics of probe replacement and the enzymology of cleavage. Previously, we have described the activity and specificity of seven structure-specific 5′ nucleases under conditions of limiting enzyme and excess substrate (*13*). This paper continues the characterization of the FEN1 enzymes from *Archaeoglobus fulgidus* (AfuFEN) and *Methanococcus jannaschii* (MjaFEN) and the DNA polymerase I homologues from *Thermus aquaticus* (TaqPol) and *Thermus thermophilus* (TthPol) under conditions of limiting target. We describe a model for the invasive signal amplification reaction and test it with the four 5′ nuclease enzymes. The model predicts that the temperature optimum for the invasive signal amplification reaction should occur near the melting temperature of the probe. In accordance with this prediction, we observed that increasing the length of the probe increases the optimum reaction temperature.

The model also predicts that increasing the concentration of the probe will increase the rate of the reaction, which we also find to be true. We also examined the ability of the enzymes to cleave under conditions in which the upstream oligonucleotide cycles instead of the probe. The FEN1 enzymes, but not TaqPol and TthPol, are able to support a high level of cleavage under these conditions. We find that the proposed model explains some, but not all, aspects of the reaction. The experimental data suggest that the kinetics of probe replacement are affected by the type of 5′ nuclease and its concentration; this effect is not accounted for in the current model. Finally, we examined the cleavage of several nonspecific substrates that are expected to generate background in the cycling reaction. By examining cleavage of these nonspecific substrates, we are able to quickly evaluate the suitability of enzymes for use in assay applications.

MATERIALS AND METHODS

Materials. Chemicals and buffers were from Fisher Scientific unless otherwise noted.

Purification of Enzymes. Structure-specific 5′ nucleases from *Thermus thermophilus*, *Thermus aquaticus*, *Archaeoglobus fulgidus*, and *Methanococcus jannaschii* were cloned, expressed, purified, and quantitated as described (*9, 13*) using His Bind resin metal chelation chromatography (Novagen) as a final step. All enzymes were dialyzed and stored in 50% glycerol, 20 mM Tris-HCl, pH 8, 50 mM KCl, 0.5% Tween 20, 0.5% Nonidet P40, 100 μg/mL BSA. A conserved aspartic acid at position 785 of TaqPol and position 787 of TthPol was mutated to an asparagine to create polymerase-deficient versions of the enzymes used in this study (*13*).

Substrate Preparation. All oligonucleotides were synthesized on a PerSeptive Biosystems instrument using standard phosphoramidite chemistries (Glen Research). The oligonucleotides labeled on their 5′ ends with TET (Glen Research) were purified by reverse-phase HPLC using a Resource Q column (Amersham-Pharmacia Biotech). All oligonucleotides were purified on a 20% denaturing polyacrylamide gel followed by excision and elution of the major band (*13*). Oligonucleotide concentrations were determined by measuring their absorption at 260 nm.

Invasive Signal Amplification Reactions with a Cycling Probe. The biotin-labeled substrates were incubated with a 5-fold excess of streptavidin (Promega) in reaction buffer containing 10 mM MOPS, pH 7.5, 0.05% Tween 20, 0.05% NP-40 and 10 μg/mL tRNA at room temperature for 10 min before assembling the reaction samples. Unless otherwise indicated, 10 μL reactions contained 2 μM probe, 0.2 nM target strand, varying amounts of enzyme, and 4 mM $MgCl_2$ in the reaction buffer described above. The reactions were assembled on ice and initiated by transferring the samples to a Mastercycler gradient thermocycler (Eppendorf). The reactions were performed at different temperatures and stopped by cooling the samples in an ice bath followed by addition of 10 μL of 95% formamide containing 10 mM EDTA and 0.02% methyl violet (Sigma). The samples were analyzed by electrophoresis through a 20% denaturing polyacrylamide gel, and then the gels were scanned on an FMBIO-100 fluorescence gel scanner (Hitachi) as described (*13*). The fraction of cleaved product was determined from intensities of bands corresponding to uncut and cut probe

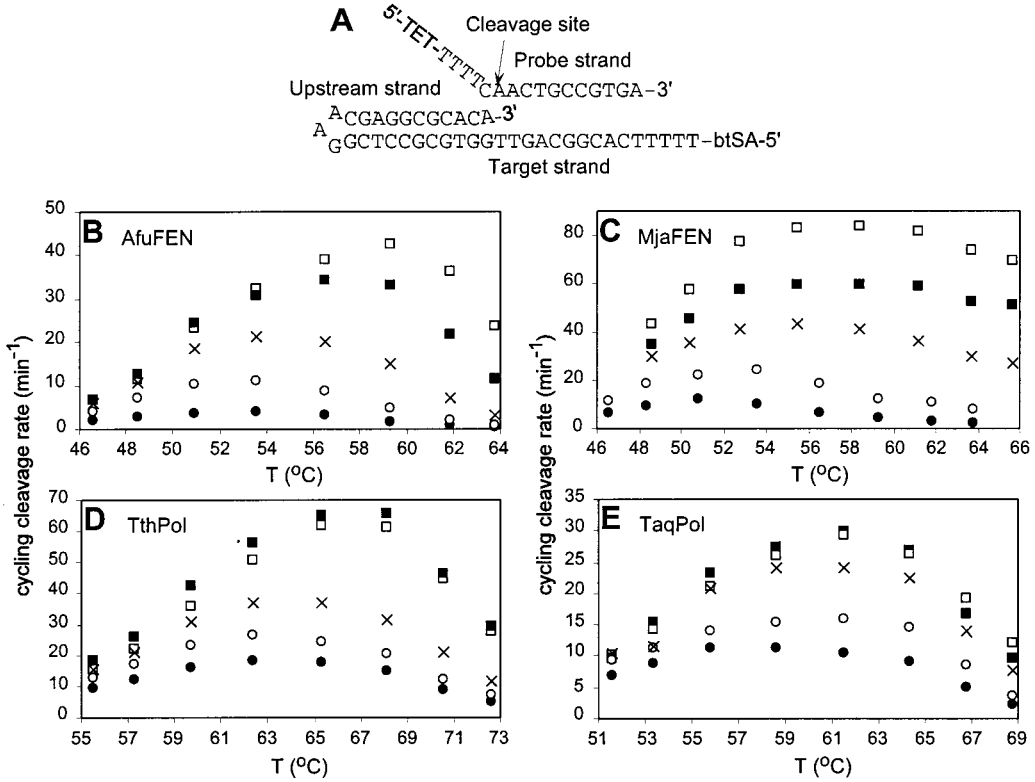

FIGURE 1: Effect of enzyme concentration and temperature on the cycling cleavage rate. (A) Sequence and proposed structure of the overlapping substrate, which consists of an integrated upstream strand and target strand (IT molecule) and a separate probe strand. Position of the cleavage site is shown by an arrow. The 5′ end of the IT molecule is modified with biotin and blocked with streptavidin (btSA) as described under Materials and Methods to prevent nonspecific 5′ nuclease cleavage of the target strand. (B−E) Cycling cleavage rate measured as a function of temperature with 2 μM downstream probe and 0.2 nM IT molecule as described under Materials and Methods. Enzyme concentrations tested: (B) (●) 4, (○) 16, (×) 64, (■) 256, and (□) 512 nM AfuFEN; (C) (●) 8, (○) 32, (×) 128, (■) 256, and (□) 512 nM MjaFEN; (D) (●) 1, (○) 2, (×) 4, (■) 16, and (□) 32 nM TthPol; (E) (●) 4, (○) 8, (×) 16, (■) 32, and (□) 64 nM TaqPol. Each experiment was repeated in triplicate, and the mean value was used for data analysis. The experimental error of the measurements did not exceed 10%.

with FMBIO Analysis software (version 6.0, Hitachi). The reactions were run so that the fraction of cut product did not exceed 20% to ensure that measurements approximated initial cleavage rates. The cycling cleavage rate was defined as the concentration of cut product divided by the target concentration and the time of the reaction (in minutes).

Reactions with a Cycling Upstream Oligonucleotide. Assays were performed using 2 μM probe/target molecule (Figure 6A) and 0.2 or 10 nM upstream oligonucleotide with 256 nM AfuFEN or 16 nM TthPol, respectively, as described above for the invasive signal amplification reactions with a cycling probe.

Michaelis−Menten Kinetics with All-in-One Substrate. The initial cleavage rate of the all-in-one substrate (Figure 5A) with 5 pM AfuFEN was measured as a function of the substrate concentration (10, 20, 40, 80, and 160 nM) and temperature (48.4, 50.8, 53.6, 56.5, 59.3, and 61.8 °C). The fraction of cleaved product was determined as described above. The cleavage rate was defined as the number of substrate molecules cut per enzyme molecule per minute.

Reactions with Nonspecific Substrates. The cycling cleavage rates with the nonoverlapping substrate (Figure 7C) were measured as described for the invasive signal amplification reactions except that the concentration of the target strand was 10 nM. The downstream duplex and X-structure substrates (Figure 7B,D) were prepared with equimolar amounts of each strand. The cleavage rates of the downstream duplex and X-structure substrates were measured at different temperatures under conditions of substrate excess (2 μM) and limiting enzyme concentration as indicated in the figure legends. The reaction products were separated on 17.5% denaturing polyacrylamide gel. The cleavage rates of the downstream duplex and X-structure substrate were defined as the number of substrate molecules cut per enzyme molecule per minute.

RESULTS

Theoretical Analysis of the Invasive Signal Amplification Reaction. An overlapping substrate for the structure-specific 5′ nucleases, described previously (*13*), consists of the target, upstream, and downstream (probe) strands as shown in Figure 1A. The target and upstream strands are joined with a stable three-nucleotide loop to maintain stoichiometry and to stabilize the binding of the upstream strand. In this substrate, the upstream and probe strands overlap by one nucleotide, although the 3′ terminal nucleotide of the upstream strand is unpaired, thus creating positional rather than sequence overlap with the annealed portion of the probe. It has previously been demonstrated that the 3′ nucleotide of the upstream oligonucleotide need not base pair to support cleavage (*9*, *12*, *13*). The 5′ nuclease cuts specifically between the first two base pairs of the duplex formed by the probe and target strands, releasing the 5′ arm of the probe and one additional nucleotide from the base-paired region.

When operated as a signal amplification reaction, the invasive cleavage is carried out under conditions in which the probe is present in large molar excess over the target strand. If the reaction is performed at elevated temperatures, the cut probe spontaneously dissociates after cleavage, thereby allowing its replacement with an uncut probe under isothermal conditions initiating a new cycle of the reaction. The upstream oligonucleotide does not need to be cycled, so it is designed to have a higher melting temperature than the probe.

With some simplification, the invasive signal amplification reaction, also referred to as the probe cycling reaction for this discussion, can be considered as a typical enzymatic reaction in which a complex formed between the 5′ nuclease, E, target, T, and upstream oligonucleotide, I, called the EIT complex, plays the role of an enzyme. The probe, P, serves as the substrate, and the reaction can be described by the following kinetic model:

$$\mathrm{EIT} + \mathrm{P} \underset{k_{-1}}{\overset{k_1}{\leftrightarrow}} \mathrm{EITP} \xrightarrow{k_h} \mathrm{EITP'} + \mathrm{A} \xrightarrow{k_2} \mathrm{EIT} + \mathrm{P'} + \mathrm{A} \quad (1)$$

where P′ is the cleaved probe, A is the cleaved 5′ arm of the probe, and EITP and EITP′ are complexes between EIT and uncut and cut probes, respectively; k_1 and k_{-1} are the association and dissociation rate constants of the probe binding with the EIT complex, respectively; k_h is the cleavage rate constant, and k_2 is the dissociation rate constant of the cleaved probe.

Several assumptions are included in the proposed model (eq 1): (i) all target molecules are assumed to be bound to the upstream oligonucleotide and enzyme, thus the kinetics of EIT formation are not included in the model; (ii) dissociation of P′ does not require prior dissociation of the enzyme from the EITP′ complex, which simplifies the model by omitting the following pathway of P′ dissociation: EITP′ ↔ E + ITP′ → EIT + P′; (iii) dissociation of P′ occurs only by the dissociative mechanism (*20*), where the cleaved probe completely dissociates before another probe anneals. The contribution from the sequential displacement mechanism (*20*), where the cleaved probe is replaced by a partially annealed uncut probe, is considered negligible. We also assume that (iv) only a small fraction of the total amount of the probe is cleaved by the enzyme, so that at any moment the concentration of P is much higher than the concentration of P′; therefore, the reverse process of the reaction, EIT + P′ → EITP′, is not taken into account.

The model summarized by eq 1 can be further described by the following equations:

$$\begin{aligned} \frac{d[\mathrm{EIT}]}{dt} &= -k_1[\mathrm{EIT}][\mathrm{P}] + k_{-1}[\mathrm{EITP}] + k_2[\mathrm{EITP'}] \\ \frac{d[\mathrm{EITP'}]}{dt} &= k_h[\mathrm{EITP}] - k_2[\mathrm{EITP'}] \\ \frac{d[\mathrm{A}]}{dt} &= k_h[\mathrm{EITP}] \end{aligned} \quad (2)$$

where the brackets are used to indicate concentrations. Additional equations can be obtained using steady-state approximations: $d[\mathrm{EIT}]/dt = 0$ and $d[\mathrm{EITP'}]/dt = 0$, and a target conservation condition: $[\mathrm{EIT}]_0 = [\mathrm{EIT}] + [\mathrm{EITP}] + [\mathrm{EITP'}]$, where $[\mathrm{EIT}]_0$ is the initial concentration of EIT.

According to assumptions (i) and (iv) discussed above, $[\mathrm{EIT}]_0 = [\mathrm{T}]_0$ and $[\mathrm{P}] = [\mathrm{P}]_0$, where $[\mathrm{T}]_0$ and $[\mathrm{P}]_0$ are the initial concentrations of the target and probe, respectively, and eqs 2 can be analytically solved to find the initial cleavage rate of the reaction:

$$\frac{d[\mathrm{A}]}{dt} = \frac{k_1[\mathrm{P}]_0[\mathrm{T}]_0}{\left(1 + \frac{k_{-1}}{k_h}\right) + k_1[\mathrm{P}]_0\left(\frac{1}{k_h} + \frac{1}{k_2}\right)} \quad (3)$$

Equation 3 can be rewritten as

$$\frac{d[\mathrm{A}]}{dt} = \alpha[\mathrm{T}]_0 \quad (4)$$

where α is the cycling cleavage rate defined as the number of probe molecules cleaved per target molecule per unit of time:

$$\alpha = \frac{k_1[\mathrm{P}]_0}{\left(1 + \frac{k_{-1}}{k_h}\right) + k_1[\mathrm{P}]_0\left(\frac{1}{k_h} + \frac{1}{k_2}\right)} \quad (5)$$

Effect of Temperature and Enzyme Concentration on the Cycling Cleavage Rate. The substrate shown in Figure 1A was used as a model substrate to study the probe cycling reaction with two archaeal FEN1 5′ nucleases (*11*), AfuFEN and MjaFEN, and two eubacterial enzymes, TaqPol and TthPol. The upstream oligonucleotide and target were combined into one molecule, called an IT molecule; its 5′ end was blocked with a biotin-streptavidin complex. The blocking group was used to prevent 5′ nuclease cleavage of the IT molecule (*10, 21*). The biotin-streptavidin complex was separated from the downstream duplex by a four nucleotide linker (5′-TTTT) to eliminate its effect on cleavage reaction. Figures 1B through 1E depict cycling cleavage rate data for the probe cycling reaction with the model substrate (Figure 1A) measured as a function of enzyme concentration and temperature for each of the four enzymes.

Two major observations can be made from these data: first, for each enzyme and each enzyme concentration, there is an optimal temperature where the cycling cleavage rate reaches a maximum; second, the cycling cleavage rate increases with enzyme concentration, either reaching a maximum for TaqPol and TthPol or approaching a plateau for AfuFEN and MjaFEN. These features of the probe cycling reaction will be analyzed in terms of the proposed kinetic model (eq 1) in the following sections.

Optimal Temperature of the Probe Cycling Reaction Correlates with the Probe Melting Temperature. The existence of an optimal temperature for the probe cycling reaction (Figure 1) can be explained by analyzing eq 5 under conditions in which the reaction temperature is either below or above the melting temperature, T_m, of the probe. For this analysis, we need to evaluate the parameters of eq 5, k_h, $k_1[\mathrm{P}]_0$, k_{-1}, and k_2, that define α. The cleavage rate constant k_h estimated for the 5′ nucleases studied in this work increases less than 10-fold in the temperature range from 50 to 75 °C (*13*), and its value varies in the range from 2 to

40 s^{-1} (ref 13, and data shown below). The association rate constant k_1 for oligonucleotides depends weakly on temperature, and its value is between 10^6 and 10^7 M^{-1} s^{-1} under conditions similar to those used in this work (*22*). This allows an estimation of the parameter $k_1[P]_0$ value as 2−20 s^{-1} assuming that $[P]_0 = 2$ μM. In contrast to the parameters k_h and $k_1[P]_0$, the dissociation rate constants k_{-1} and k_2 for oligonucleotides should depend dramatically on temperature (*23, 24*). Therefore, at temperatures below T_m, k_{-1}, $k_2 \ll k_h$, $k_1[P]_0$, whereas above the probe's T_m the opposite would be true, k_{-1}, $k_2 \gg k_h$, $k_1[P]_0$.

According to this analysis, below the T_m of the probe, eq 5 is reduced to

$$\alpha = k_2 \tag{6}$$

In other words, below T_m, the reaction rate should be limited by the low dissociation rate constant k_2 for the cleaved probe. Above T_m, eq 5 can be transformed into

$$\alpha = \frac{k_h k_1 [P]_0}{k_{-1}} \tag{7}$$

where α becomes limited now by a high dissociation rate constant, k_{-1}, or by a low probability, $k_1[P]_0/k_{-1}$, of probe binding. This analysis suggests that the optimal reaction temperature should correspond to conditions where the association rate $k_1[P]_0$ and the dissociation rate constant k_2 are equal or close to each other or, in other words, the optimal probe cycling reaction temperature should be close to the probe's melting temperature.

The proposed relationship between the optimal reaction temperature and the probe's melting temperature can be tested using probes with different length and, therefore, different T_ms. Figure 2 shows the temperature dependence of the cycling cleavage rate for 12-, 13-, and 15-nucleotide probes with the same target molecule for AfuFEN and TthPol. As expected, the longer probes have higher optimal reaction temperatures under the same experimental conditions for both enzymes. The experimentally determined optimal temperatures for 12-, 13-, and 15-nucleotide probes with 256 nM AfuFEN (Figure 2B) are 57.5, 58, and 64 °C, respectively. The melting temperatures for these probes can be predicted using nearest-neighbor thermodynamic parameters (*25*). The unknown thermodynamic parameters for DNA duplex formation in buffers containing Mg^{2+} and 5′ nucleases were substituted with the available parameters for Na^+ by selecting an appropriate Na^+ concentration (*26*). We found that the nearest-neighbor parameters for 500 mM Na^+ predict melting temperatures of 57.3, 58.6, and 64.2 °C for the 12-, 13-, and 15-nucleotide cleaved probes, respectively, which are in excellent agreement with the corresponding experimentally determined optimal temperatures. The optimal reaction temperatures with 16 nM TthPol (Figure 2C) are approximately 8 °C higher than those observed with 256 nM AfuFEN. Figure 2B shows that the maximal value of α for AfuFEN increases with probe length, although for TthPol the maximal cycling cleavage rate for the 15-nucleotide probe is 30% lower than that obtained for the 12- and 13-nucleotide probes.

Effect of 5′ Nucleases on the Probe Cycling Reaction. The increase in the cycling cleavage rate with increasing enzyme concentration (Figure 1) can be explained by saturation of the substrate complex with enzyme. At enzyme concentrations corresponding to the plateau or to maximal levels of the cycling cleavage rate, it is assumed that all target molecules are bound to the enzyme (see the first assumption for eq 1). As shown in Figure 1, the saturating concentrations for the TaqPol and TthPol enzymes are approximately 1 order of magnitude lower than for the AfuFEN and MjaFEN enzymes, suggesting that TaqPol and TthPol bind the substrate more strongly than do the FEN1 enzymes.

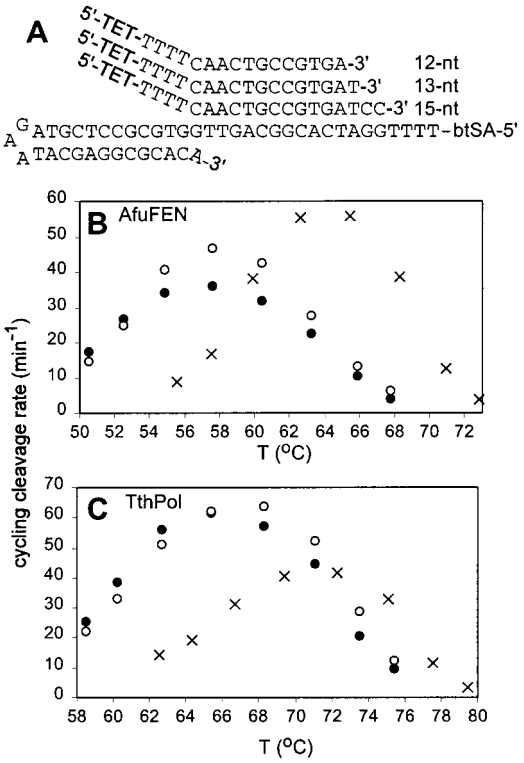

FIGURE 2: Effect of temperature on the cycling cleavage rate for 12-, 13-, and 15-nucleotide probes with AfuFEN or TthPol. (A) Sequence and proposed structure of the target molecule and 12-, 13-, and 15-nucleotide probes used in the probe cycling reaction. (B) Cycling cleavage rate as a function of temperature for (●) 12-, (○) 13-, and (×) 15-nucleotide probe (2 μM) with 0.2 nM target molecule and 256 nM AfuFEN. (C) Same conditions as (B) except with 16 nM TthPol. Each experiment was repeated in triplicate, and the mean value was used for data analysis. The experimental error of the measurements did not exceed 10%.

If cleavage occurs much faster than probe dissociation, or the cleavage rate constant k_h is much higher than the dissociation rate constants k_{-1} and k_2, $k_h \gg k_{-1}$, k_2, then according to eq 5:

$$\alpha = \frac{k_1 [P]_0}{1 + \frac{k_1}{k_2}[P]_0} \tag{8}$$

wherein α is expected to be enzyme-independent. The data shown in Figure 1 are not consistent with this conclusion. First, the maximal cycling cleavage rate and the corresponding reaction temperature differ for the four enzymes used in this work. Second, the optimal reaction temperature for each 5′ nuclease increases significantly with increasing enzyme concentration. These observed influences of the enzymes on the cycling cleavage rate imply that the association rate

constant k_1 and/or dissociation rate constants k_{-1} and k_2 depend on both the type of 5′ nuclease and its concentration.

Effect of Probe Concentration on the Cycling Cleavage Rate. Equation 5 can be rewritten using the Michaelis−Menten formalism:

$$\alpha = \frac{\alpha_{max}[P]_0}{K_m + [P]_0} \quad (9)$$

where K_m is the Michaelis constant for probe cycling reaction:

$$K_m = \frac{k_2(k_h + k_{-1})}{k_1(k_h + k_2)} \quad (10)$$

and α_{max} is the maximal cycling cleavage rate:

$$\alpha_{max} = \frac{k_2 k_h}{k_2 + k_h} \quad (11)$$

Using the analysis applied above for the discussion of the temperature effect on α, we assume that below the T_m of the probe, $k_h \gg k_2, k_{-1}$, and eqs 9 and 10 can be reduced to: $K_m = k_2/k_1$ and $\alpha_{max} = k_2$. Above the T_m, $k_2, k_{-1} \gg k_h$, and the same equations yield: $K_m = k_{-1}/k_1$, $\alpha_{max} = k_h$. In summary, this analysis predicts that K_m should increase sharply with temperature in the entire temperature range, similar to the dissociation rate constants k_{-1} and k_2, whereas α_{max} should have a similar strong temperature dependence only below T_m and a moderate temperature dependence defined by the cleavage rate constant k_h, above T_m.

To determine K_m and α_{max} for the substrate shown in Figure 1A, the cycling cleavage rate was measured as a function of probe concentration and temperature for 256 nM AfuFEN and 16 nM TthPol (Figure 3). The K_m and α_{max} values were determined from a double-reciprocal plot of $1/\alpha$ versus $1/[P_0]$ (data not shown) and plotted as a function of temperature for both enzymes in Figure 4. In agreement with the theoretical model, the measured K_m value increases sharply with temperature for each enzyme throughout the entire temperature range. The α_{max} values for AfuFEN and TthPol reach plateaus of 70 and 100 min^{-1}, respectively, after an initial sharp increase below the optimal reaction temperature. The steep decline in α_{max} above the optimal temperature cannot be explained in terms of the model described in this work, because the model predicts a moderate increase in α_{max} above the optimal temperature.

Kinetic Analysis of 5′ Nuclease Activity under Enzymatic Conditions. Analysis of 5′ nuclease activity under typical enzymatic conditions of limiting enzyme and excess substrate allows an estimation of the cleavage rate constant, k_h, and equilibrium dissociation constant, K_d, of the enzyme−substrate complex. For this purpose, we used an overlapping substrate, called the all-in-one substrate (Figure 5A), that has the upstream and downstream strands linked to the target strand with stable three-nucleotide loops (*13*). Since the probe does not cycle on this substrate, the enzymatic cleavage rate is defined as the number of all-in-one substrate molecules cleaved per enzyme molecule per minute, which is different from the cycling cleavage rate. Cleavage of the all-in-one substrate (Figure 5A), also termed the PIT substrate, can be described by the following model:

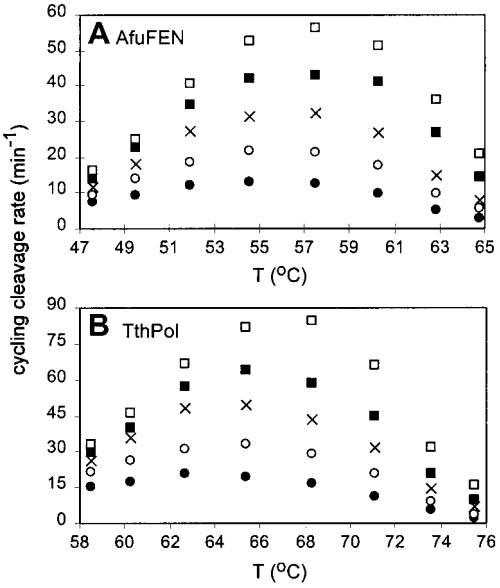

FIGURE 3: Cycling cleavage rate for a 12-nucleotide probe with AfuFEN or TthPol as a function of temperature for different probe concentrations. (A) Cycling cleavage rate for the invasive substrate shown in Figure 1A was measured with (●) 0.32, (○) 0.64, (×) 1.28, (■) 2.56, and (□) 5 μM probe, 0.2 nM target molecule, and 256 nM AfuFEN as described under Materials and Methods. (B) Same conditions as (A) except with 16 nM TthPol. Each experiment was repeated in triplicate, and the mean value was used for data analysis. The experimental error of the measurements did not exceed 10%.

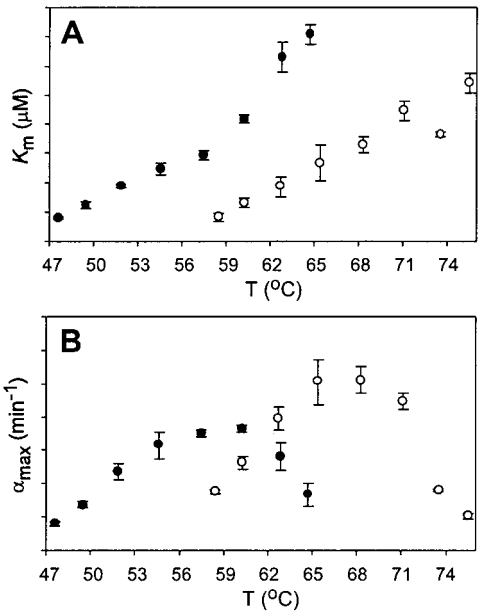

FIGURE 4: Effect of temperature on K_m and α_{max} of the probe cycling reaction with AfuFEN or TthPol. (A) Effect of temperature on the Michaelis constant K_m of the probe cycling reactions shown in Figure 3 for (●) 256 nM AfuFEN and (○) 16 nM TthPol. (B) Temperature dependence of the maximal cycling cleavage rate α_{max} determined from the data shown in Figure 3 for (●) 256 nM AfuFEN and (○) 16 nM TthPol.

$$E + PIT \underset{m_{-1}}{\overset{m_1}{\rightleftarrows}} EPIT \xrightarrow{m_h} EP'IT + A \xrightarrow{m_2} E + P'IT + A \quad (12)$$

where m_1 and m_{-1} are the association and dissociation rate constants of enzyme binding with PIT, respectively, m_h is the enzymatic cleavage rate constant, and m_2 is the dissociation rate constant for the enzyme and cleaved substrate, P′IT.

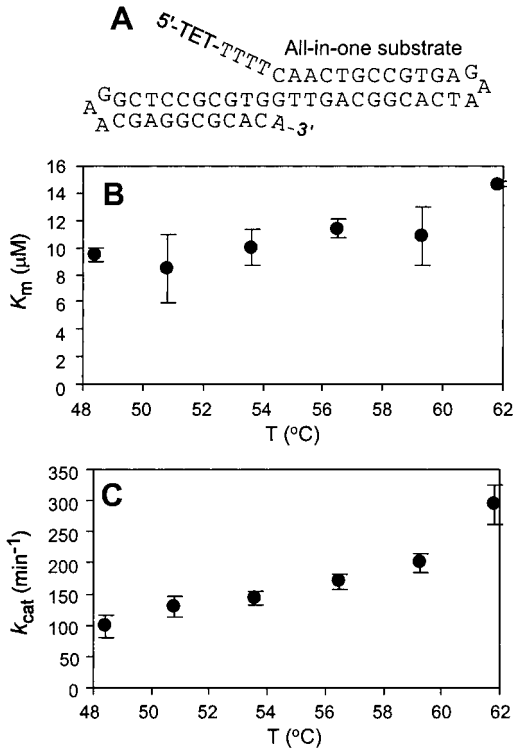

FIGURE 5: Effect of temperature on K_m and k_{cat} for AfuFEN with the all-in-one substrate under enzymatic conditions. (A) Sequence and proposed structure of the all-in-one substrate. (B) The Michaelis constant K_m of AfuFEN with the all-in-one substrate as a function of temperature. (C) Temperature dependence of the maximal catalytic rate constant k_{cat} of AfuFEN with the all-in-one substrate. Reactions with the all-in-one substrate were performed as described under Materials and Methods.

By analogy with the model proposed by eq 1, the Michaelis constant, K_m, and the maximal catalytic rate, k_{cat}, of a reaction performed under enzymatic conditions are given by (compare with eqs 10 and 11)

$$K_m = \frac{m_2(m_h + m_{-1})}{m_1(m_h + m_2)} \quad (13)$$

and

$$k_{cat} = \frac{m_2 m_h}{m_2 + m_h} \quad (14)$$

The initial enzymatic cleavage rates for AfuFEN with the all-in-one substrate (PIT) were measured as a function of substrate concentration and temperature as described under Materials and Methods, and the experimental data were used to determine the K_m and k_{cat} of AfuFEN (Figure 5B,C). According to eq 13, a K_m value of 10−14 nM (Figure 5B) can be used to estimate the equilibrium dissociation constant, $K_d = m_{-1}/m_1$, of AfuFEN, assuming that $m_2 \cong m_{-1}$. The k_{cat} value of 100−300 min^{-1} (Figure 5C) can serve as a lower limit estimate of m_h (eq 14). The m_h value can be used to estimate the cleavage rate constant, k_h, of the probe cycling reaction (eq 1), although these two rate constants cannot be considered the same due to differences in the conditions of the corresponding reactions. We were not able to determine a K_m value for TthPol using cleavage kinetics of the all-in-one substrate and obtained only an upper limit estimate of 1 nM (data not shown).

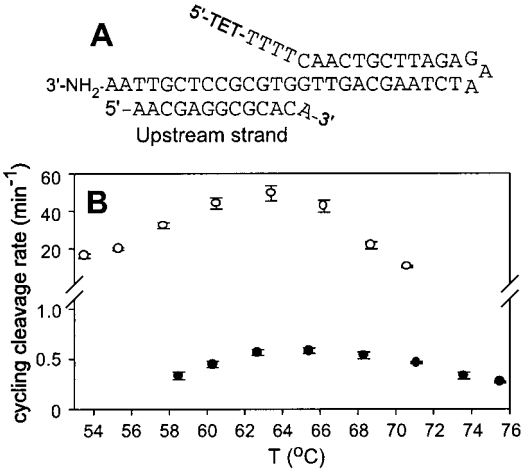

FIGURE 6: Cycling cleavage rate in a cycling upstream oligonucleotide reaction with AfuFEN or TthPol. (A) Sequence and proposed structure of the substrate for the upstream oligonucleotide cycling reaction. (B) Cycling cleavage rate of the upstream oligonucleotide cycling reaction with (○) 256 nM AfuFEN and (●) 16 nM TthPol as a function of temperature. The reaction conditions are described under Materials and Methods.

Invasive Signal Amplification Reaction with a Cycling Upstream Oligonucleotide. To investigate the alternative variant of the invasive signal amplification reaction with a cycling upstream oligonucleotide, we used an overlapping substrate that consists of the upstream oligonucleotide I and the PT molecule formed by the target T and the probe P, as shown in Figure 6A. Signal amplification in this design is achieved by cleavage of multiple PT molecules in the presence of limiting upstream oligonucleotide under conditions favorable for its rapid turnover. As with the substrate shown in Figure 1A, the cycling cleavage rate α is defined analogously as the number of PT probes cut per upstream oligonucleotide per minute. The cycling cleavage rate of this reaction with AfuFEN and TthPol was plotted as a function of temperature in Figure 6B. Comparing Figures 1 and 6 shows that the reactions with cycling probe and cycling upstream oligonucleotide have similar cycling cleavage rates with AfuFEN, but for TthPol, the reaction with the cycling upstream oligonucleotide has a value of α almost 2 orders of magnitude lower than the value of α for the alternative design. The greatly reduced turnover rate of the upstream oligonucleotide with TthPol suggests that the upstream oligonucleotide cannot be released fast enough after cleavage to ensure a high cycling rate of the probe.

Substrate Specificity as an Important Factor in Choosing an Enzyme for the Invasive Signal Amplification Reaction. Specific recognition of the overlapping substrate by the structure-specific 5′ nucleases (*9*, *12*, *13*) is a critical feature for their application to nucleic acid analysis. To determine the specificity of the 5′ nucleases, the activities of each enzyme with three nonspecific substrates (Figure 7B−D) that are likely to be formed during an invasive signal amplification reaction on complex DNA samples (e.g, human genomic DNA) have been determined and compared with cleavage of the specific overlapping substrate. The downstream duplex substrate (Figure 7B) can form when the probe binds to a target DNA molecule at a site with partial homology to the

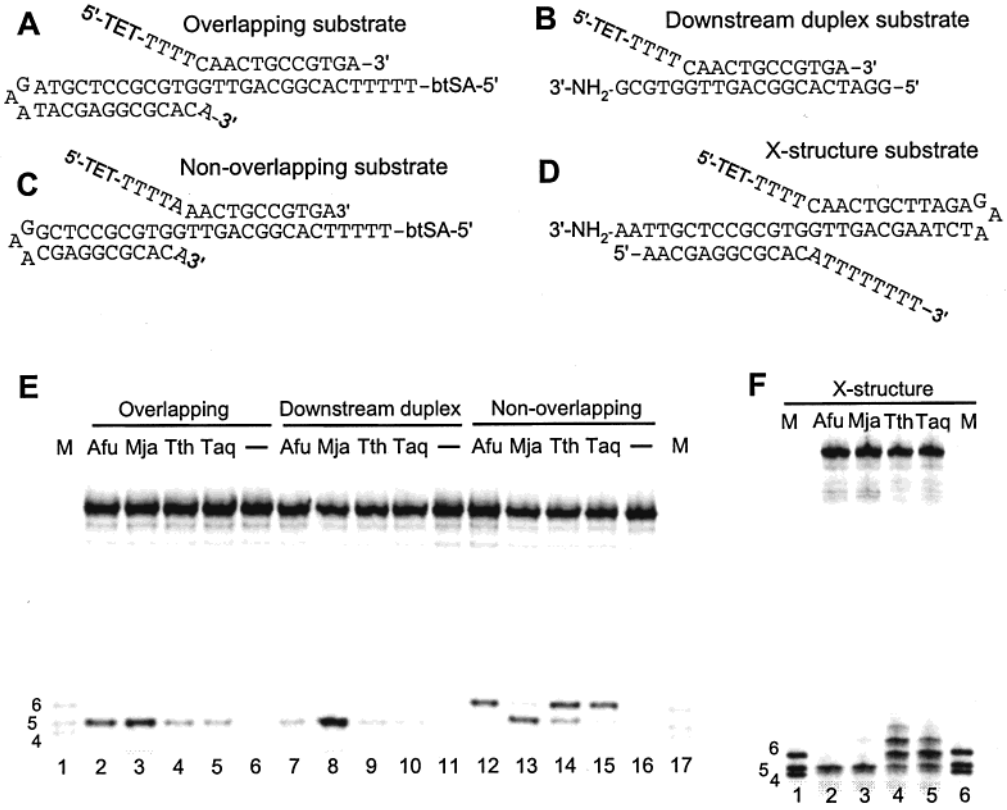

FIGURE 7: Specificity of AfuFEN, MjaFEN, TthPol, and TaqPol. Sequence and proposed structure of the (A) overlapping, (B) downstream duplex, (C) nonoverlapping, and (D) X-structure substrates. (E) Lanes 2−5, products of the overlapping substrate cleavage (2 μM probe, 0.2 nM target strand) with 256 nM AfuFEN, 256 nM MjaFEN, 32 nM TthPol, and 32 nM TaqPol, respectively, at 57 °C for 30 min; lanes 7−10, products of the downstream duplex substrate cleavage (2 μM each strand) with 256 nM AfuFEN (32 h), 256 nM MjaFEN (10 min), 256 nM TthPol (16 h), and 256 nM TaqPol (16 h) at 53 °C; lanes 12−15, products of the nonoverlapping substrate cleavage (2 μM probe, 20 nM target strand) with 256 nM AfuFEN (1 h), 256 nM MjaFEN (30 s), 32 nM TthPol (1 h), and 32 nM TaqPol (1 h) at 51 °C; lanes 1 and 17, mixture of 5′-TTTTCA, 5′-TTTTC, and 5′-TTTT size markers labeled with TET dye at the 5′ end; lanes 6, 11, and 16, no enzyme controls for each substrate. (F) Lanes 2−5, products of the X-structure substrate cleavage (2 μM each strand) with 256 nM AfuFEN (60 min), 4 nM MjaFEN (10 min), 64 nM TthPol (60 min), and 32 nM TaqPol (60 min) at 63 °C; lanes 1 and 6 show the size markers. The reactions were performed as described under Materials and Methods.

intended target sequence in the absence of the upstream oligonucleotide. For 12-nucleotide probes, the average number of such sites on human genomic DNA would be approximately 400. The nonoverlapping substrate (Figure 7C) is typical for mutation detection using the invasive cleavage reaction (*9*, *14*, *15*) and corresponds, for example, to a mutant probe annealed to a wild target. For the best mutation discrimination, the probe is usually designed so that the mutation eliminates a base pair at the end of the downstream duplex, and the nonoverlapping substrate therefore lacks overlap between the upstream oligonucleotide and probe. For the X-structure (Figure 7D), which resembles the double flap structure previously described (*27*), a major nonspecific substrate of the secondary invasive reaction in the cascade invasive signal amplification reaction (*14*, *15*) is formed between uncut probe and secondary target. The characteristic feature of the X-structure is the long noncomplementary 3′ arm of the upstream oligonucleotide.

Figure 7E demonstrates that all enzymes cut the downstream duplex substrate mostly at the same site as the overlapping substrate, producing a 5-nucleotide product. The X-structure is cut 5 nucleotides from the 5′ end of the probe with AfuFEN and MjaFEN, while TthPol and TaqPol generate a major product of 6 nucleotides and two minor products of 5 and 7 nucleotides (Figure 7F). The cleavage products of the nonoverlapping substrate with MjaFEN, TthPol, and TaqPol produce both 5- and 6-nucleotide 5′ products, whereas AfuFEN generates only a 6-nucleotide product. The enzymatic cleavage rates for the downstream duplex and X-structure substrates were measured under conditions of limiting enzyme, whereas the cycling cleavage rates for the overlapping and nonoverlapping substrates were determined under conditions of limiting target as described under Materials and Methods. The cleavage rates for all substrates were determined as a function of temperature (data not shown); maximal cleavage rates as well as the corresponding optimal temperatures are summarized in Table 1.

DISCUSSION

We have investigated the activity of four thermostable structure-specific 5′ nucleases from the Archaea and Eubacteria in the invasive signal amplification (probe cycling) reaction. Contrary to other probe cycling techniques (*6*−*8*), the invasive cleavage reaction requires annealing of two oligonucleotides, rather than one, to a target nucleic acid molecule. This property greatly increases the assay specificity with complex DNA samples but still allows the use of relatively short probes at moderately high temperatures. Two important parameters of any signal amplification reaction are target specific signal generation and background, which is defined as any signal generated in the absence of the specific target. Together, these two parameters define the signal:

Table 1: Cleavage Rates of the Overlapping, Downstream Duplex, Nonoverlapping, and X-Structure Substrates with AfuFEN, MjaFEN, TthPol, and TaqPol at Optimal Temperatures

	overlapping substrate,[a] min^{-1}	downstream duplex,[b] min^{-1}	nonoverlapping,[c] min^{-1}		X-structure,[d] min^{-1}
			5 nt	6 nt	
AfuFEN	34	0.0001	ND	0.1	0.06
MjaFEN	60	1.6	21	−	8
TthPol	66	0.002	0.2	0.2	0.3
TaqPol	30	0.001	0.02	0.1	0.6

[a] Cycling cleavage rates of the overlapping substrate with 256 nM AfuFEN at 56 °C, 256 nM MjaFEN at 56 °C, 16 nM TthPol at 67 °C, and 32 nM TaqPol at 62 °C from Figure 1. [b] Cleavage rates of the downstream duplex substrate (2 μM) shown in Figure 7B with AfuFEN at 56 °C, MjaFEN at 56 °C, TthPol at 67 °C, and TaqPol at 62 °C. [c] Cycling cleavage rates of the nonoverlapping substrate (2 μM probe, 0.01 μM target) shown in Figure 7C with 256 nM AfuFEN at 56 °C, 256 nM MjaFEN at 56 °C, 32 nM TthPol at 67 °C, and 32 nM TaqPol at 62 °C. Two rates, corresponding to the 5- or 6-nucleotide products, are shown. ND: cleavage was not detectable. [d] Cleavage rates of the X-structure substrate (2 μM) with AfuFEN, MjaFEN, TthPol, and TaqPol at 63 °C.

background ratio and ultimately the limit of detection of the assay. We will focus this discussion on the factors that affect the cycling cleavage rate and the background generation in an invasive signal amplification reaction.

Higher cycling cleavage rates can be achieved merely by choice of enzyme. MjaFEN has roughly a 2-fold greater cycling cleavage rate than AfuFEN, and TthPol has a 2-fold greater cleavage rate than TaqPol. For each enzyme, the cycling cleavage rate increases with increasing enzyme concentration, presumably due to the target becoming saturated with enzyme. At the higher enzyme concentrations, the cycling cleavage rate plateaus for TthPol and TaqPol and approaches a plateau for the FEN1 enzymes. This saturation effect suggests that for the best performance of the assay, each enzyme has an optimal concentration above which the increase in the cycling rate does not compensate for the increase in nonspecific reactions producing the background. The optimal enzyme concentration is expected to be an order of magnitude higher for the FEN1 enzymes than for TthPol and TaqPol (Figure 1), which can be explained by the lower equilibrium dissociation constants, K_d, for the TthPol and TaqPol enzymes, most likely due to the presence of the polymerase domain, which the FEN1 5′ nucleases lack. The reported K_d values of 7.5 nM for the archaeal FEN1 homologue, human FEN1 (*28*), and 0.2 nM for the TaqPol and TthPol homologue, *E. coli* PolI (*29*, *30*), support this hypothesis. In this work, we estimated the K_d values for AfuFEN and TthPol with the all-in-one substrate (Figure 5) as 8−14 nM and <1 nM, respectively, which are consistent with the published data.

Increasing the probe concentration is another way to increase the cycling cleavage rate (Figure 3). Analysis of the results shown in Figure 3 using Michaelis−Menten formalism gives a maximal cycling cleavage rate, α_{max}, of 70 and 100 min^{-1} for AfuFEN and TthPol, respectively (Figure 4B). To reach this maximal rate, the reaction requires a relatively high probe concentration, because the K_m values corresponding to the optimal reaction conditions are 1.5−2 μM (Figure 4A). According to eq 10, the K_m for the probe cycling reaction is inversely proportional to the association rate constant, k_1, of the probe. Thus, the same cycling cleavage rate can be achieved at lower probe concentrations by increasing the association rate constant of duplex formation. Factors known to increase the association rate constant of nucleic acids include increasing ionic strength (*31*), the presence of polycations, the presence of certain detergents (*32*), and certain nucleic acid modifications (*33*), all of which could be tested for their effect on the invasive signal amplification reaction.

To determine which factors affect background generation in the invasive signal amplification reaction, we have studied the activity of the enzymes with nonspecific substrates that typically arise during the course of the reaction (Figure 7). The downstream duplex substrate, for instance, mimics the case in which the probe anneals in the absence of the upstream oligonucleotide to sites that share sequence similarity with the intended target sequence. We have observed much greater variability in the cleavage rate for the enzymes when they cleave the downstream duplex substrate versus the overlapping substrate (Table 1). For example, AfuFEN cuts the downstream duplex substrate 16 000-fold more slowly than does MjaFEN. Such a low cleavage rate serves to decrease background significantly, more than compensating for the 2-fold lower cycling cleavage rate relative to MjaFEN, and makes AfuFEN a far better choice for a practical detection assay (data not shown). Another DNA structure that can contribute to background is the X-structure substrate that arises when the invasive signal amplification reaction is set up as a cascade of two reactions (*14*, *15*). The secondary reaction in the cascade utilizes a combined probe/target (PT) molecule, similar to that shown in Figure 6A. In the cascade, the cleaved 5′ arm of the target-specific probe molecule of the primary reaction becomes the upstream oligonucleotide in a secondary invasive reaction. However, this means that the uncleaved primary probe can also anneal to the PT molecule, thus creating an X-structure (Figure 7D). The presence of the upstream oligonucleotide in the X-structure, even with a long unpaired 3′ arm, significantly increases the nonspecific activity of the enzymes compared to the downstream duplex substrate (Table 1). Comparison of the specific and nonspecific activities among the four enzymes predicts that AfuFEN would have the best signal: noise ratio in the invasive signal amplification reaction.

We have utilized the unique specificity of the 5′ nucleases to create a signal amplification assay specifically for the purpose of mutation detection (*9*, *14*). We have found that the enzymes display the greatest mutation discrimination when the upstream oligonucleotides and probes are designed so that the mutation is present immediately upstream of the cleavage site of the probe (data not shown). When a wild-type probe hybridizes to a mutant target, there is no overlap between the upstream oligonucleotide and probe, resulting in a greatly reduced cleavage rate for all enzymes. We observe that AfuFEN has the highest ratio, 340:1, of activity on the overlapping and nonoverlapping substrates among all four enzymes. The actual mismatch specificity may be even higher, because AfuFEN cleaves the nonoverlapping substrate one nucleotide downstream from the normal site of cleavage (Figure 7E, lane 12), a property that could be used in the assay design (*9*, *14*, *15*) to improve its specificity. The high level of mutation discrimination observed with the invasive cleavage reaction is due to the exquisite specificity of the 5′ nucleases, rather than to the reduced duplex stability

caused by a mismatch. Indeed, if the lower stability, and therefore a lower optimal reaction temperature, of the nonoverlapping probe were the only parameter affecting the cycling cleavage rate, it could only account for mutation discrimination of a factor of only 1.5 (data not shown).

One goal of this work was to develop a theoretical model of the invasive signal amplification reaction. The model proposed in this work correctly describes important characteristics of the reaction, such as the dependence of the cycling cleavage rate on temperature and enzyme concentration (Figure 1), the correlation between the optimal reaction temperature and probe's melting temperature (Figure 2), and the effect of probe concentration on the cycling cleavage rate (Figure 3). Conversely, we have observed effects that are not consistent with the model. For example, the increase in the optimal reaction temperature with increasing enzyme concentration and different optimal temperatures observed for all enzymes (Figure 1) suggest that the 5′ nucleases stabilize the duplex formed between the probe and the target strands. The increased duplex stability in the presence of the 5′ nucleases could be a result of accelerated enzyme-catalyzed annealing between the probe and target. Such a mechanism has been previously described for the phage T4 gene 32 protein and the *E. coli* single-strand binding protein (*34*, *35*).

The data gathered in this work do not definitively answer the question as to which part of the invasive signal amplification reaction—probe cleavage or probe replacement—defines its rate-limiting step. The fact that the characteristics of the reaction are unique for each enzyme (Figure 1) argues that the rate-limiting step is enzyme-dependent. On the other hand, the cleavage rate constant k_h is generally much higher than the maximal cycling cleavage rate α_{cat}. For example, k_h and α_{cat} for AfuFEN have been estimated as >150 min^{-1} (Figure 5C) and 70 min^{-1} (Figure 4B) at the optimal temperature, respectively, suggesting that cleavage is faster than the overall rate of the reaction. The strong dependence of the cycling cleavage rate on probe concentration (Figure 3) further supports the idea that probe replacement is slower than cleavage. In conclusion, we propose the hypothesis that the rate-limiting step of the invasive signal amplification reaction is controlled by the kinetics of probe replacement, although the 5′ nucleases affect the kinetics of probe association and/or dissociation. Examples of such interference possibly include the decreased cycling cleavage rate of the 15-nucleotide probe with TthPol (Figure 2C) despite increased enzymatic cleavage rate at higher temperatures (*13*) and a very low cycling cleavage rate in the TthPol reaction with the cycling upstream oligonucleotide (Figure 6B). Further investigations are in progress to better define the rate-limiting steps in the invasive signal amplification reaction.

ACKNOWLEDGMENT

We thank Peggy Eis, Robert Kwiatkowski, Luis Reynaldo, and Kafryn Lieder for critically reading the manuscript and discussions.

REFERENCES

1. Mullis, K. B., and Faloona, F. A. (1987) *Methods Enzymol. 155*, 335−350.
2. Wu, D. Y., and Wallace, R. B. (1989) *Genomics 4*, 560−569.
3. Kwoh, D. Y., Davis, G. R., Whitfield, K. M., Chappelle, H. L., DiMichele, L. J., and Gingeras, T. R. (1989) *Proc. Natl. Acad. Sci. U.S.A. 86*, 1173−1177.
4. Urdea, M. S., Running, J. A., Horn, T., Clyne, J., Ku, L. L., and Warner, B. D. (1987) *Gene 61*, 253−264.
5. Stollar, B. D., and Rashtchian, A. (1987) *Anal. Biochem. 161*, 387−394.
6. Duck, P., Alvarado-Urbina, G., Burdick, B., and Collier, B. (1990) *BioTechniques 9*, 142−148.
7. Copley, C. G., and Boot, C. (1992) *BioTechniques 13*, 888−892.
8. Okano, K., and Kambara, H. (1995) *Anal. Biochem 228*, 101−108.
9. Lyamichev, V., Mast, A. L., Hall, J. G., Prudent, J. R., Kaiser, M. W., Takova, T., Kwiatkowski, R. W., Sander, T. J., de Arruda, M., Arco, D. A., Neri, B. P., and Brow, M. A. (1999) *Nat. Biotechnol. 17*, 292−296.
10. Lyamichev, V., Brow, M. A., and Dahlberg, J. E. (1993) *Science 260*, 778−783.
11. Harrington, J. J., and Lieber, M. R. (1994) *EMBO J. 13*, 1235−1246.
12. Lyamichev, V., Brow, M. A., Varvel, V. E., and Dahlberg, J. E. (1999) *Proc. Natl. Acad. Sci. U.S.A. 96*, 6143−6148.
13. Kaiser, M. W., Lyamicheva, N., Ma, W., Miller, C., Neri, B., Fors, L., and Lyamichev, V. I. (1999) *J. Biol. Chem. 274*, 21387−21394.
14. Kwiatkowski, R. W., Lyamichev, V., de Arruda, M., and Neri, B. P. (1999) *Mol. Diagn. 4*, 353−364.
15. Hall, J. G., Eis, P. S., Law, S. M., Reynaldo, L. P., Prudent, J. R., Marshall, D. J., Allawi, H. T., Mast, A. L., Dahlberg, J. E., Kwiatkowski, R. W., de Arruda, M., Neri, B. P., and Lyamichev, V. I. (2000) *Proc. Natl. Acad. Sci. U.S.A.* (in press).
16. Hall, J., Breitzman, R., Wood, N., Kwiatkowski, R., Hennesy, K., Vavra, S., Rosenblate, H., Silver, A., and Fagan, E. A. (1998) *Hepatology 98*, 583A.
17. Griffin, T. J., Hall, J. G., Prudent, J. R., and Smith, L. M. (1999) *Proc. Natl. Acad. Sci. U.S.A. 96*, 6301−6306.
18. Ryan, D., Nuccie, B., and Arvan, D. (1999) *Mol. Diagn. 4*, 135−144.
19. Mein, C. A., Barratt, B. J., Dunn, M. G., Siegmund, T., Smith, A. N., Esposito, L., Nutland, S., Stevens, H. E., Wilson, A. J., Phillips, M. S., Jarvis, N., Law, S., de Arruda, M., and Todd, J. A. (2000) *Genome Res. 10*, 330−343.
20. Reynaldo, L. P., Vologodskii, A. V., Neri, B. P., and Lyamichev, V. I. (2000) *J. Mol. Biol. 297*, 511−520.
21. Murante, R. S., Rust, L., and Bambara, R. A. (1995) *J. Biol. Chem. 270*, 30377−30383.
22. Williams, A. P., Longfellow, C. E., Freier, S. M., Kierzek, R., and Turner, D. H. (1989) *Biochemistry 28*, 4283−4291.
23. Porschke, D., and Eigen, M. (1971) *J. Mol. Biol. 62*, 361−381.
24. Craig, M. E., Crothers, D. M., and Doty, P. (1971) *J. Mol. Biol. 62*, 383−401.
25. Allawi, H. T., and SantaLucia, J., Jr. (1997) *Biochemistry 36*, 10581−10594.
26. Nakano, S., Fujimoto, M., Hara, H., and Sugimoto, N. (1999) *Nucleic Acids Res. 27*, 2957−2965.
27. Harrington, J. J., and Lieber, M. R. (1995) *J. Biol. Chem. 270*, 4503−4508.
28. Nolan, J. P., Shen, B., Park, M. S., and Sklar, L. A. (1996) *Biochemistry 35*, 11668−11676.
29. Astatke, M., Grindley, N. D., and Joyce, C. M. (1995) *J. Biol. Chem. 270*, 1945−1954.
30. Minnick, D. T., Astatke, M., Joyce, C. M., and Kunkel, T. A. (1996) *J. Biol. Chem. 271*, 24954−24961.
31. Ross, P. D., and Sturtevant, J. M. (1960) *Proc. Natl. Acad. Sci. U.S.A. 46*, 1360−1365.
32. Pontius, B. W., and Berg, P. (1991) *Proc. Natl. Acad. Sci. U.S.A. 88*, 8237−8241.
33. Young, S., and Wagner, R. W. (1991) *Nucleic Acids Res. 19*, 2463−2470.
34. Alberts, B. M., and Frey, L. (1970) *Nature* 227, 1313−1318.
35. Christiansen, C., and Baldwin, R. L. (1977) *J. Mol. Biol. 115*, 441−454.

BI0007829